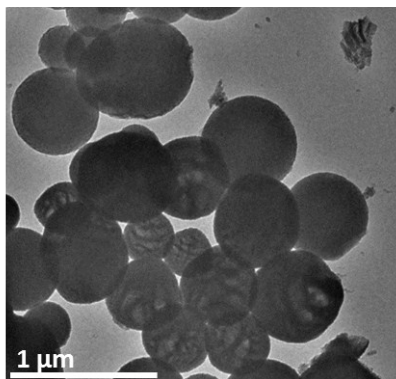


## **Supporting Information**

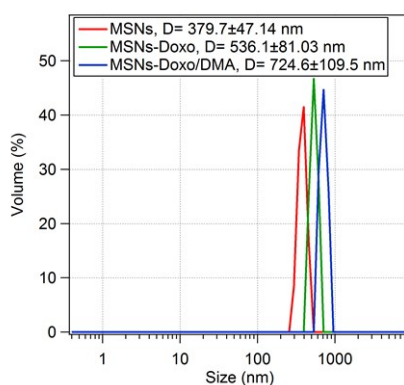
### **Boosting the therapeutic efficiency of nanovectors: exocytosis engineering**

Stefania Corvaglia<sup>1,2</sup>, Daniela Guarnieri<sup>1</sup>, and Pier Paolo Pomba<sup>1,2\*</sup>

a) TEM image



b) DLS



c) Z-Potential

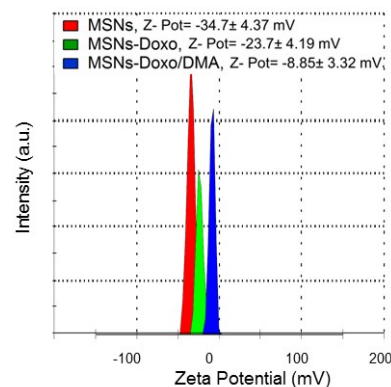


**Figure S1.** (a) Representative transmission electron microscopy (TEM) image of bare MSNs; (b) Dynamic light scattering (DLS) of MSNs, MSNs-Doxo and MSNs-Doxo/DMA in water; (c) Zeta-potential of the 3 nanosystems. A slight increase in the average particles diameter was observed after Doxo and Doxo-DMA loading, indicative of partial particle agglomeration after functionalization, due to the less negative surface charge of MSNs. Z-potential changes also confirmed successful loading.

Nanocarrier	Doxo ( $\mu\text{g/ml}$ )	DMA ( $\mu\text{g/ml}$ )
MSNs-Doxo	3.94 $\pm$ 0.36	
MSNs-DMA		2.35 $\pm$ 0.34
MSNs-Doxo/DMA	4.05 $\pm$ 0.09	2.85 $\pm$ 0.65

**Table S1.** Concentrations of the molecules loaded in the MSN nanocarriers (10  $\mu\text{g/ml}$ ) in the different formulations. The Doxo concentration is identical in the two MSNs-Doxo and MSNs-Doxo/DMA systems.

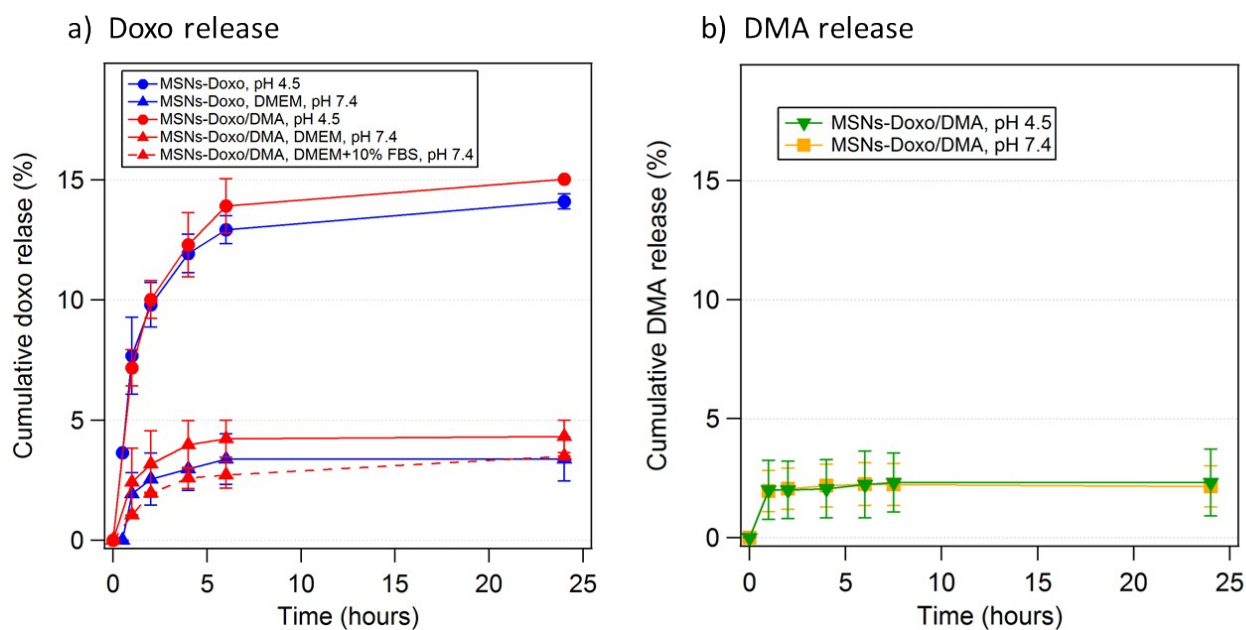


**Figure S2.** Doxo (a) and DMA (b) release from the co-loaded nanocarrier (MSNs-Doxo/DMA) and from the MSNs-Doxo alone. The release was tested in aqueous solutions mimicking the cellular (DMEM pH 7.4, or DMEM + 10% FBS, pH 7.4) and lysosomal (citrate buffer pH 4.5) environments. As expected, Doxo release was pH-dependent (higher drug release at acidic pH), while DMA seemed to be not affected by pH variations. Importantly, the Doxo release was the same in the two nanoformulations (i.e., with or without the DMA co-loading).

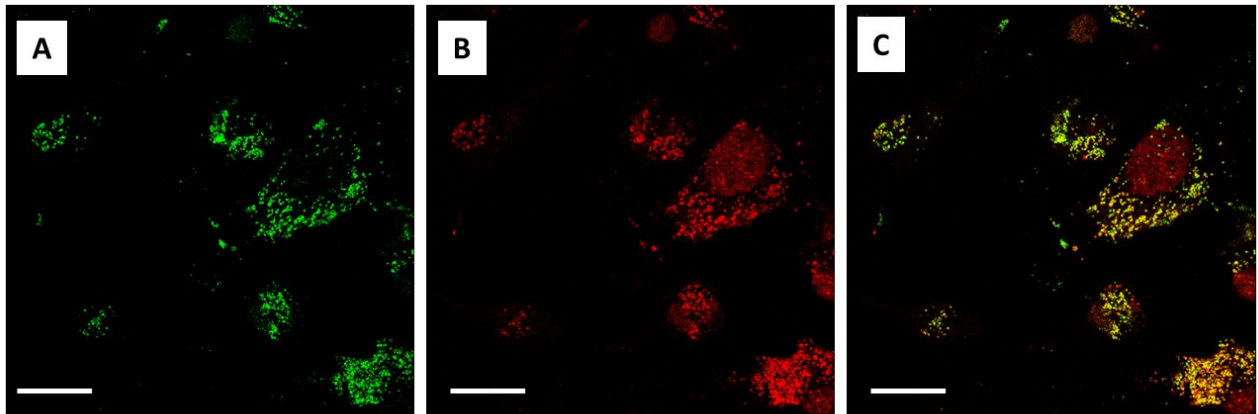


**Figure S3.** Co-localization analysis of MSNs with lysosomes in HeLa cells after 4 hour incubation (in these experiments we used MSNs loaded with doxorubicin to exploit its intrinsic fluorescence for imaging). Confocal microscopy images show (a) lysosomes stained with LysoTracker in green, (b) the intrinsic fluorescence signal of Doxorubicin loaded into MSNs in red, and (c) merged image of the two channels. An almost total co-localization of MSNs-Doxo with lysosomes was observed (yellow signal). Some doxorubicin fluorescence can be also observed into cell nucleus because of the partial drug release from the nanovectors. Scale bar 25  $\mu\text{m}$ .

<b>Pearson's coefficient</b>	<b>Manders' coefficient</b> (fraction of Doxo overlapping LysoTracker)
0.82 ± 0.03	0.83 ± 0.06

**Table S2.** Pearson's and Manders' coefficient values calculated by JACoP ImageJ plugin, indicating the degree of co-localization between doxorubicin and LysoTracker. Data are reported as mean value ± the standard deviation (SD).

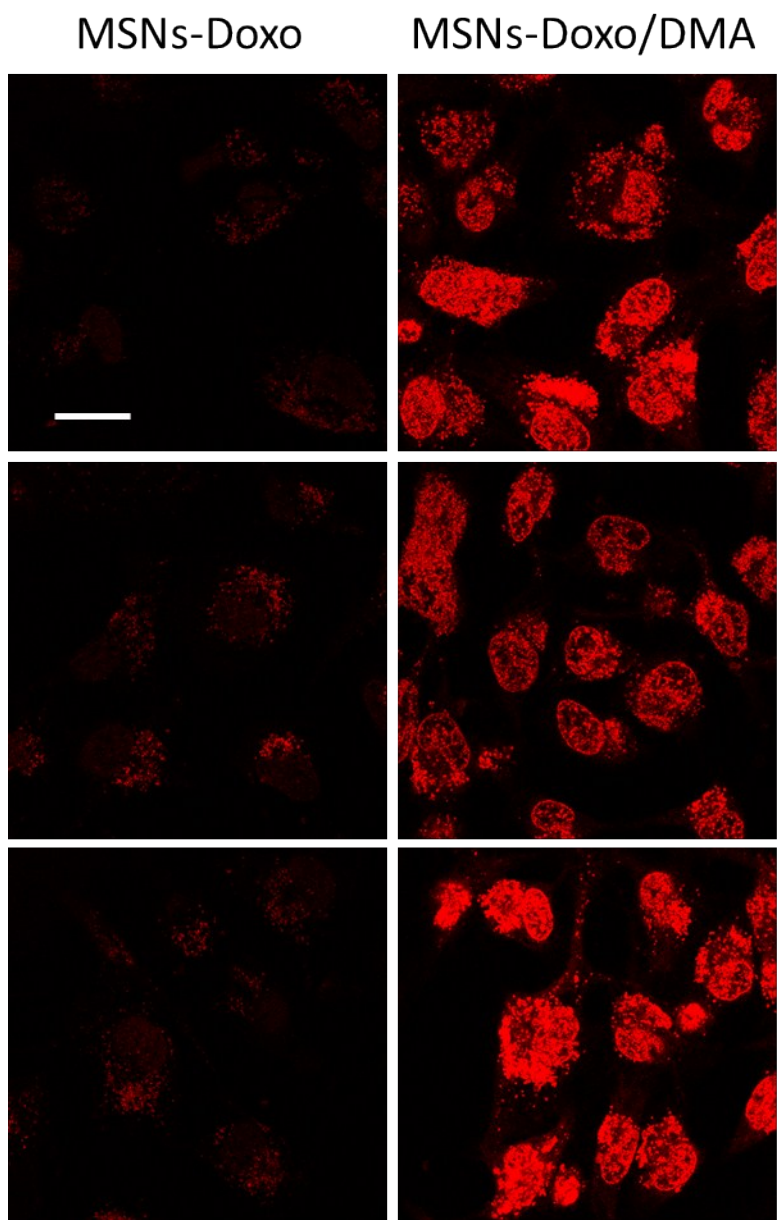


**Figure S4.** The same confocal microscopy images reported in Fig. 3 in the main text, acquired with lower settings so to avoid signal saturation in the right panels. The images show Doxorubicin distribution in HeLa cells, treated with 10  $\mu\text{g}/\text{mL}$  MSNs-Doxo (left panels) and MSNs-Doxo/DMA (right panels), after 4 hours of incubation. Scale bar 25  $\mu\text{m}$ .

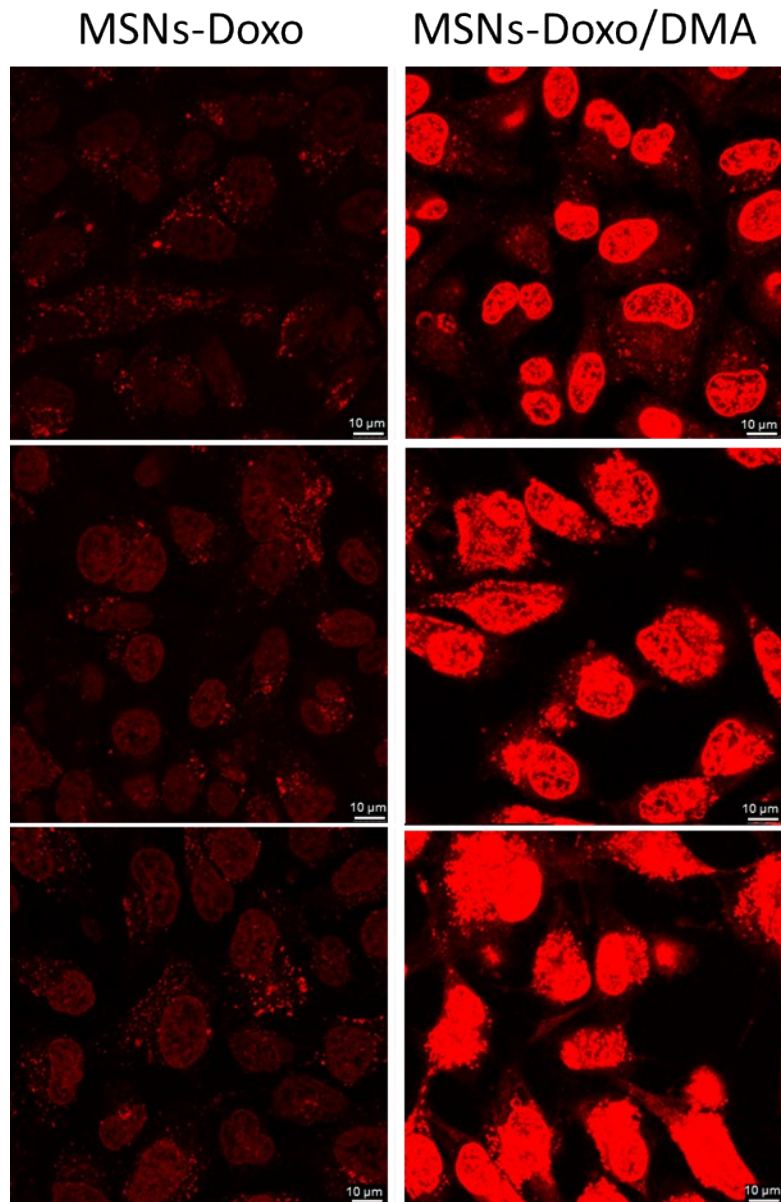


**Figure S5.** Additional confocal microscopy images of Doxorubicin distribution in HeLa cells, treated with 10 μg/mL MSNs-Doxo (left panels) and MSNs-Doxo/DMA (right panels), after 4 hours of incubation.

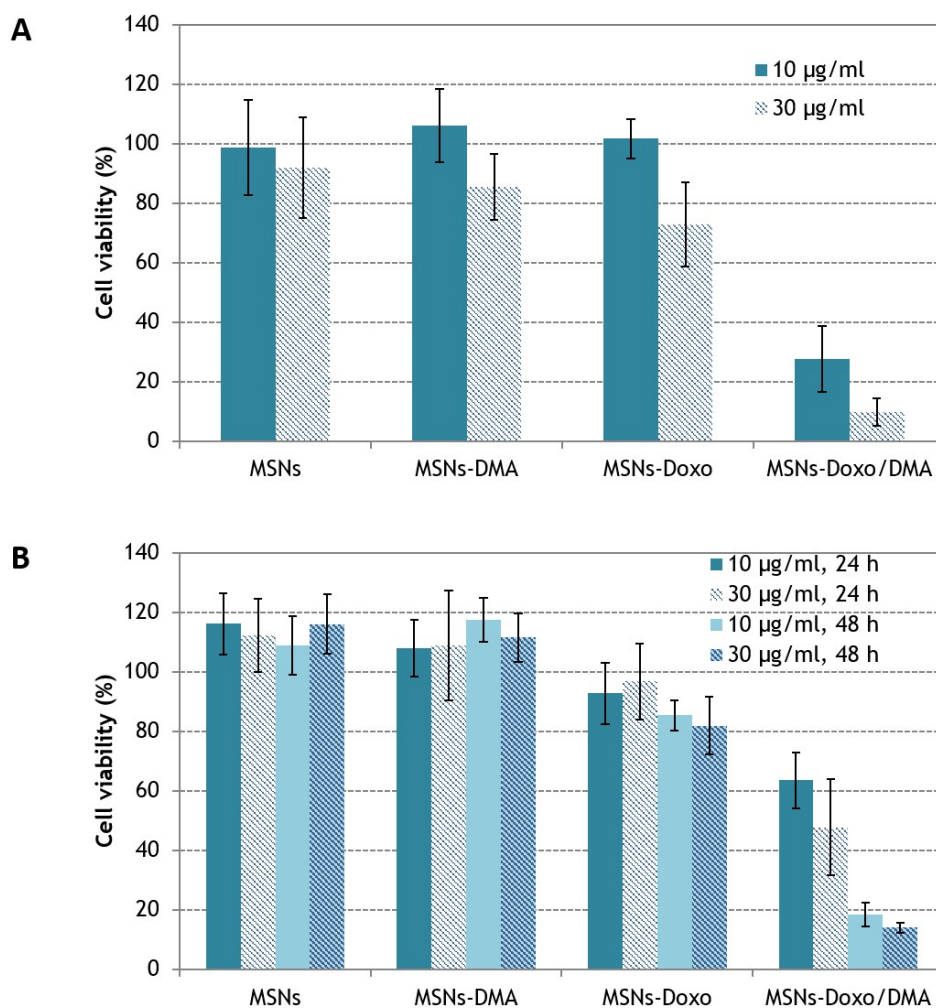


**Figure S6.** WST-8 cell viability assay of the different nanoformulations (MSNs-Doxo and MSNs-Doxo/DMA) on SH-5SY cells after 24 hours (A) and on A549 cells after 24 and 48 hours of incubation (B), at two MSNs concentrations (10 and 30 µg/ml), respectively corresponding to Doxo concentrations of 3.9 and 11.8 µg/ml. Bare (MSNs) and DMA-loaded (MSNs-DMA) nanovectors were also tested for comparison. A549 cells show a higher drug resistance than SH-5SY cells, reaching a similar percentage of cell mortality after longer incubation time (48 hours) (B). Data are reported as the average of six different samples and the error bars represent the standard deviation (100% viability represents non-treated control cells).



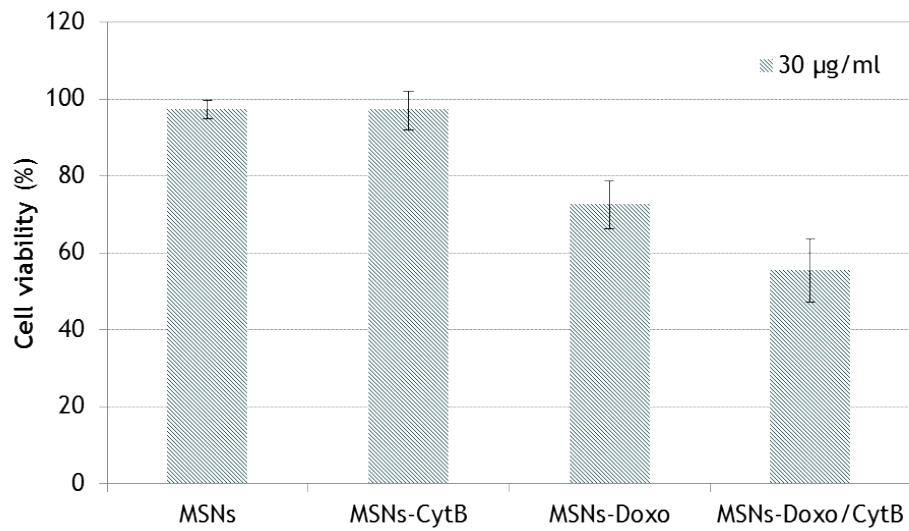


**Figure S7.** Exocytosis engineering with the inhibitor cytochalasin B (CytB). WST-8 cell viability assay of the different nanoformulations (MSNs-Doxo and MSNs-Doxo/CytB) on HeLa cells after 24 hours of incubation, at 30 µg/ml MSNs concentration. Bare (MSNs) and CytB-loaded (MSNs-CytB) nanovectors were also tested for comparison. Data are reported as the average of 16 different samples and the error bars represent the standard deviation (100% viability represents non-treated control cells).

<b>Nanomaterial</b>	<b>DLS (nm)</b>	<b>Z-pot (mV)</b>
SiO <sub>2</sub> NPs	85±4	33±4
AuNPs	64±4	-24±9

**Table S3.** DLS and Zeta-potential characterization of 50 nm amino-functionalized SiO<sub>2</sub> NPs and 65 nm citrate-capped AuNPs.

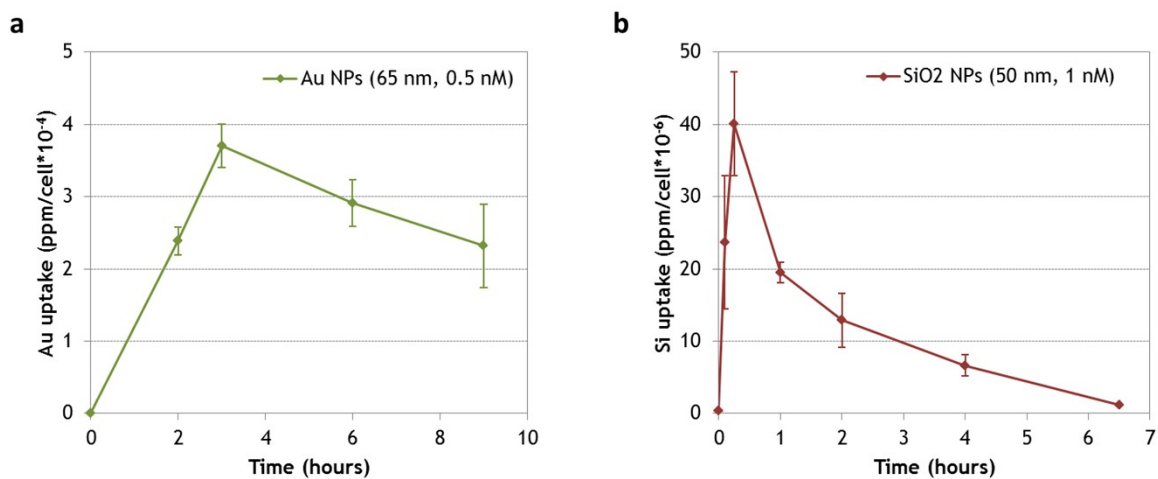


**Figure S8.** Uptake kinetics of 65 nm citrate capped gold nanoparticles (a) and 50 nm amino-functionalized silica nanoparticles (b) in HeLa cells measured by ICP-AES. The graphs report the average silica and gold content per cell, calculated as the average of three experiments. The error bars represent the standard deviations.